Hindawi Publishing Corporation
International Journal of Photoenergy
Volume 2013, Article ID 981753, 7 pages
http://dx.doi.org/10.1155/2013/981753

Methodology Report

Preparation of Fe-Doped TiO_2 Nanotubes and Their Photocatalytic Activities under Visible Light

Honghui Teng,[1,2] Shukun Xu,[1] Dandan Sun,[2] and Ying Zhang[2]

[1] *Department of Chemistry, Northeastern University, Shenyang 110004, China*
[2] *College of Environmental Science and Engineering, Jilin Normal University, Siping 136000, China*

Correspondence should be addressed to Honghui Teng; tenghonghui@jlnu.edu.cn and Shukun Xu; xushukun46@126.com

Received 18 January 2013; Revised 8 April 2013; Accepted 8 May 2013

Academic Editor: Monica Baia

Fe-doped TiO_2 nanotubes (Fe-TNTs) have been prepared by ultrasonic-assisted hydrothermal method. The structure and composition of the as-prepared TiO_2 nanotubes were characterized by transmission electron microscopy, X-ray diffraction, and UV-Visible absorption spectroscopy. Their photocatalytic activities were evaluated by the degradation of MO under visible light. The UV-visible absorption spectra of the Fe-TNT showed a red shift and an enhancement of the absorption in the visible region compared to the pure TNT. The Fe-TNTs were provided with good photocatalytic activities and photostability and under visible light irradiation, and the optimum molar ratio of Ti : Fe was found to be 100 : 1 in our experiments.

1. Introduction

Photocatalysis is a "green" technology with promising applications in a wide assortment of chemical and environmental technologies [1]. Since the photocatalytic splitting of water on TiO_2 electrodes was discovered by Fujishima and Honda in 1972, TiO_2 photocatalysis has been extensively investigated in the field of environmental protection owning to its potential in environmental problems such as air purification and wastewater treatment [2–6]. However, the TiO_2 photocatalysts were in powder form in most studies, which shows some disadvantages for practical use including the difficulties in separation or recovery from the treated water. Recently, titania nanotubes (TNTs) as photocatalyst have gained importance in wastewater treatment, they have several advantages, such as no waste solids disposal problems and utilization of sunlight or near UV light for irradiation [7], and can overcome the separation problem [8].

For improvement of photocatalytic activity of TNT and efficient utilization of solar energy, a series of metal and nonmetal doping, such as iron, nickel, platinum, chromium, carbon, nitrogen, and iodine, have been investigated for modifications of TNT [9–16]. Among of them, Fe is the most frequently investigated, and many studies have shown that the Fe-doped TNT exhibits effective photocatalytic activity for degradation of organic pollutant under visible light irradiation [8, 17–19]. Moreover, among all reported available candidates, Fe is one of the most suitable for industrial applications considering its low cost and easy preparation [20]. Doping TiO_2 with Fe^{3+} is an effective approach to reduce electron-hole recombination rate and increase photocatalytic efficiency in terms of its semifull electronic configuration and ion radius close to Ti^{4+} [20]. Xu and Yu [21] reported Fe-modified TNTs by integrating a dip-coating procedure and annealing posttreatment. The resulting Fe_2O_3-TNTs displayed a higher photoelectrocatalytic activity under visible light irradiation than pure TNTs. Fe_2O_3/TiO_2 nanorod-nanotube arrays prepared by pulsed electrodeposition technique exhibited strong absorption in the range of 200–600 nm [21].Wu and coworkers [20] prepared Fe incorporated TiO_2NTs by an ultrasound-assisted impregnating-calcination method. Fe-incorporation induced the redshift of the absorption edge of TiO_2NTs into the visible light range. An and coworkers [21–23] reported iron-coated TiO_2 nanotubes by treating hydrogen titanate nanotubes with $Fe(OH)_3$ sol. Iron-coated nanotubes exhibit better photocatalytic performance under visible light irradiation than their precursors. Tu and

coworkers [8] produced Fe-doped TiO_2 nanotube arrays by the template-based LPD method with the commercial AAO membrane as the template. The resulting Fe-TNTs exhibited good photocatalytic activities under visible light irradiation.

In this paper, we report Fe-doped titanate nanotubes by ultrasonic-assisted hydrothermal method with $Fe(NO_3)_3$ aqueous solution. It is a very simple process and does not require any special treatment that other methods need. The resulting Fe-doped TNT showed good photocatalytic activities under visible light irradiation. This work would be valuable for the practical application of TiO_2 in the field of photocatalysis under visible light irradiation.

2. Experimental Sections

2.1. Preparation of Samples. Fe-doped TNT was fabricated by using the ultrasonic-assisted hydrothermal method [24]. The anatase TiO_2 powders (40–60 nm) were employed as the Ti source, and $Fe(NO_3)_3$ aqueous solutions were used as the Fe source. In a typical procedure, 1.0 g TiO_2 powders suspensions were dispersed in 50 mL 10 M NaOH aqueous solution, 1 mL different concentrations of $Fe(NO_3)_3$ aqueous solutions (0.013, 0.063, 0.125, 0.375, and 0.625 mol/L) were separately dropped into the above alkaline solution under moderate stirring, and then 9.8 mol/L of alkaline solutions were sonicated for 12 h at temperature of 343 K to form a homogeneous solution; five different molar ratios were Ti : Fe = 100 : 5, 100 : 3, 100 : 1, 100 : 0.5, and 100 : 0.1 to produce five Fe-TNT samples, namely, Fe-TNT-5, Fe-TNT-3, Fe-TNT-1, Fe-TNT-0.5, and Fe-TNT-0.1. The resulting mixture was transferred into a stainless steel autoclave with a teflon liner, which was then sealed and maintained at 180°C for 12 h. TiO_2 suspension solution has been transformed into colloidal state by sonication, which is the precondition of synthesis of ultralong nanotube and experiment showed that it cannot form colloidal state in less than 12 h. After the hydrothermal treatment, the slurry was discharged into plastic beaker, diluted with 1 L of distilled water, and then filtrated by Buchner funnel under vacuum. The filter cake was washed with distilled water repeatedly until the pH value of the washing solution is less than 7 and then dried through vacuum freeze for 12 h. After the prepared materials were calcined at 773 K for 2 h, Fe-doped TNTs were obtained. All the chemicals were of analytical grade and used without further purification as received from Sinopharm Chemical Reagent Co., Ltd.

2.2. Samples Characterization. The morphologies of as-prepared samples were analyzed by transmission electron microscopy (TEM) (JEOL JEM-100CX II, accelerating voltage 100 kV). About 0.5 g sample was pressed in quartz glass groove, and the X-ray diffraction (XRD) patterns of the samples were measured at room temperature using Rigaku D/MAX 2500 X-ray diffractometer (CuK$\alpha\lambda$ = 0.154 nm) radiation under 40 kV and 100 mA. The UV-Vis adorable spectra of the samples were recorded with Beijing Purkinje General TU-1810UV-vis spectrophotometer.

2.3. Measurement of Photocatalytic Activity. The photocatalytic activities of the samples were evaluated by the degradation of methylorange (MO) in a cylindrical quartz vessel in response to visible light at room temperature. A type experiment was performed as follows: in a 100 mL vessel, 50 mg of the samples was dispersed in 50 mL of 20 mg/L MO aqueous solution. Before illumination, the mixtures were magnetically stirred in the dark to ensure the establishment of adsorption/desorption equilibrium of MO on the sample surfaces. Subsequently, the mixtures were irradiated with 40W tungsten lamp which is used as visible light source. The distance between the lamp and the suspension was kept at 8 cm. At given intervals, 3 mL of the suspension was sampled and subsequently centrifuged at a rate of 8000 rpm for 15 min to remove the particles of catalyst. The concentration of MO was determined by measuring the absorbance at 575 nm using a Beijing Purkinje General TU-1810 UV-vis spectrophotometer. The degradation efficiency (η) was described by the equation $\eta = (c_0 - c)/c_0 \times 100\% = (A_0 - A)/A_0 \times 100\%$ (c_0 and c were the concentrations of MO at the beginning and after the photocatalytic reaction for certain time, while A_0 and A were the absorption intensities at the beginning and after photocatalytic reaction for certain time).

3. Results and Discussion

3.1. Morphology and Structure. Figure 1 shows the TEM images of samples. Many previous papers have reported that the TNT are broken and agglomerate after calcinations at above 673 K [7]. Figure 1(a) is the TEM image of pure TNT, which shows collapse of nanotubular structure after calcination at 773 K. Compared with pure TNT, the Fe-doped TNT samples (Figures 1(b), 1(c), 1(d), 1(e), and 1(f)) still keep their nanotubular structure, and the length of the nanotubes is up to several hundreds of nanometres. Furthermore, the thickness of the wall of nanotubes increases with the increase of the doped amount of Fe, which is caused by the Fe_2O_3 particles. Similar results have been reported by An and coworkers [23]. They regarded that the insertion of Fe_2O_3 particles into the interlayer space makes the thickness of the wall of nanotubes become lager, and these particles support the nanotubular structure and make the Fe-doped TNT own thermal stability higher.

The XRD patterns of the as-prepared titanate nanotubes are shown in Figure 2. Clearly, all the curves reveal similar diffractions, and the peak positions with 2θ at 9.59°, 25.02°, 31.17°, and 48.32° are well consistent with the values of titanate nanotubes [17], which correspond with the (020), (110), (130), and (200) crystal planes, respectively. The peak positions of the pure titanate nanotubes and the Fe-doped titanate nanotubes are almost the same. No characteristic reflections of the Fe_2O_3 phases are detected with the increase of iron-doped dosage. It means that Fe^{3+} are indeed doped into the structure of titanate nanotubes, respectively, and the doping of ions Fe^{3+} does not change the structure of nanotubes obviously. Similar results have been reported in the literature on the Fe_2O_3-TiO_2 system [25, 26]. They regarded the lack of separate iron oxide phase as the incorporation of Fe^{3+} in

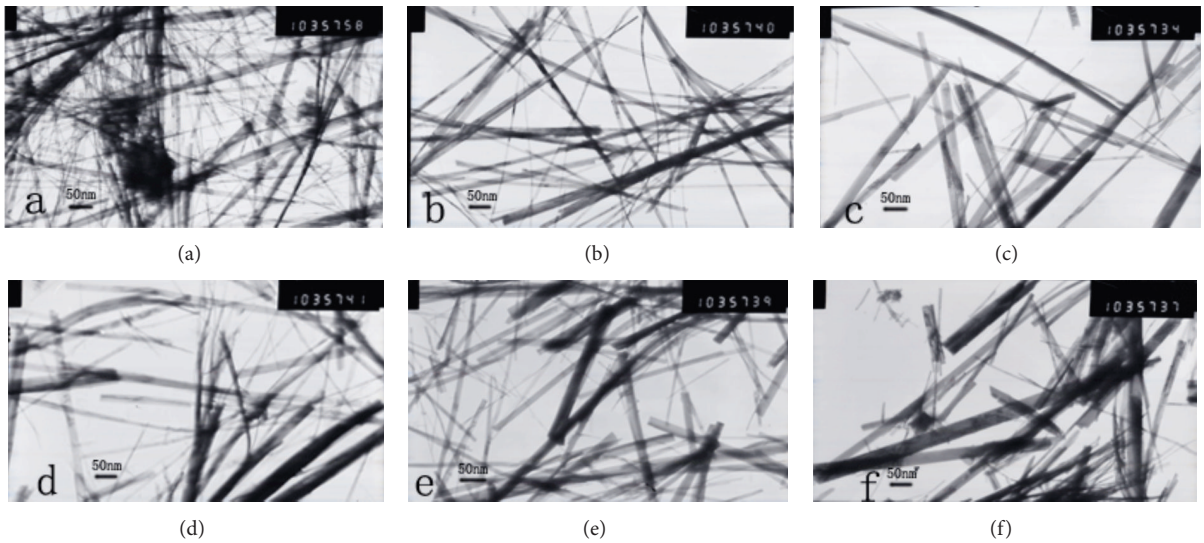

Figure 1: The TEM images of as-synthesized samples: (a) pure TNT, (b) Fe-TNT-0.1, (c) Fe-TNT-0.5, (d) Fe-TNT-1, (e) Fe-TNT-3, and (f) Fe-TNT-5.

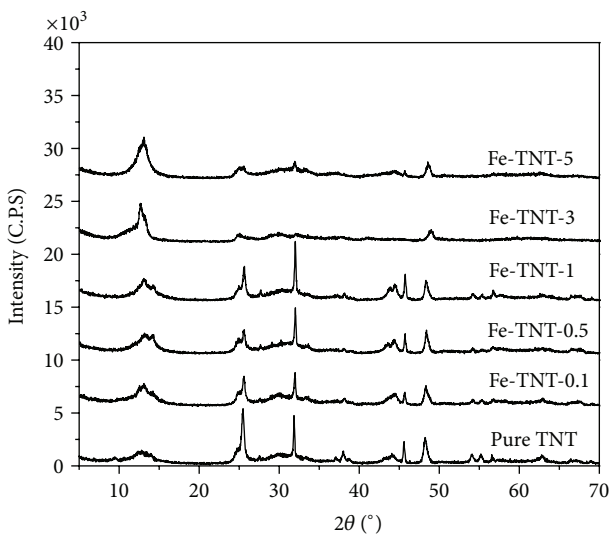

Figure 2: The XRD images of as-synthesized samples (pure TNT, Fe-TNT-0.1, Fe-TNT-0.5, Fe-TNT-1, Fe-TNT-3, and Fe-TNT-5).

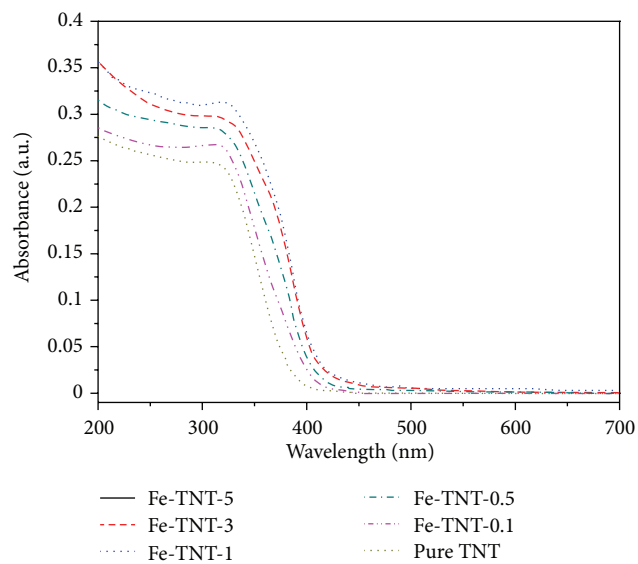

Figure 3: The UV-vis diffuse reflectance spectra of the as-synthesised samples (pure TNT, Fe-TNT-0.1, Fe-TNT-0.5, Fe-TNT-1, Fe-TNT-3, and Fe-TNT-5).

the anatase crystal structure substituting Ti^{4+} or very fine and highly dispersed in the TiO_2 nanotubes and cannot be detected by XRD.

Figure 3 shows the UV-vis diffuse reflectance spectra of as-prepared Fe-doped TNT samples and pure TNT and Fe-doped TNTs exhibit an evident red-shift and extend their absorption to the visible light region. Increasing the doped amount of Fe, the intensities between 410 and 440 nm are raised up. The red-shift can be attributed to the formation of a new dopant energy level below the conduction band for the titanate [27]. The UV-vis data reveals that the Fe-doped TNT has an Eg value which is smaller than that of pure TNT. The narrower band gap will extend the optical response to the visible region and facilitate excitation of an electron from the valence band to the conduction band, which is beneficial for the photocatalytic activity.

3.2. Photocatalytic Activity. In order to evaluate accuracy of the photocatalytic activity of the Fe-doped TNTs and to avoid affection of adsorption, adsorption/desorption equilibrium of MO on the sample surfaces was studied, and the results were shown in Figure 4. After being magnetically stirred for 10 min in the dark, the adsorption/desorption equilibrium was achieved regardless of pure TNT and Fe-doped TNTs (Figure 4(a)), or different initial pH value (2.1–7.5) of MO solution (Figure 4(b)). So, the mixtures were magnetically

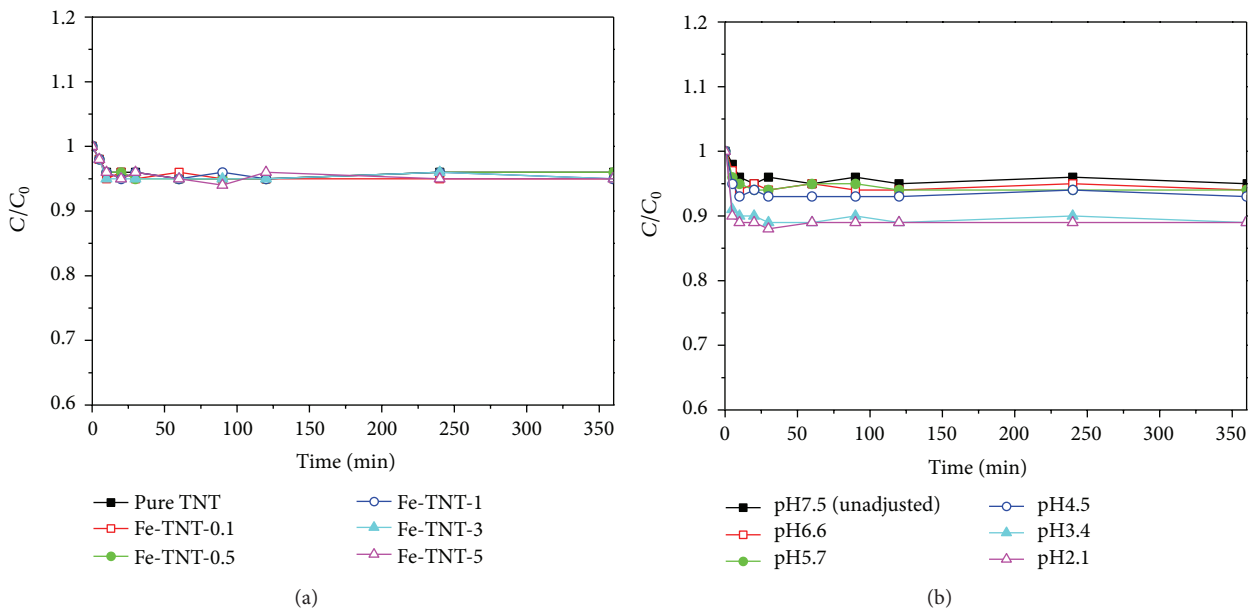

Figure 4: Adsorption/desorption equilibrium of MO on the sample surfaces ((a), different catalysts; (b), different pH) at different magnetically stirred time in the dark.

stirred for 10 min in the dark before illumination at the following experiments.

Figure 5 shows the photodegradation curves of methyl orange for Fe-doped TNTs as a function of Fe doping concentration. About 14, 28, 32, 45, 51, and 59% of the methyl orange is degraded after 1 h irradiation in the presence of pure TNT, Fe-TNT-5, Fe-TNT-3, Fe-TNT-0.1, Fe-TNT-0.5, and Fe-TNT-1, respectively. The activities of Fe-doped TNTs increase firstly with the molar ratios of Ti : Fe from 100 : 0 to 100 : 1 and then decrease when the molar ratios of Ti : Fe are further increased to 100 : 5. As the molar ratios of Ti : Fe are 100 : 1 (Fe-TNT-1), they arrives at the largest k value. All the Fe-doped samples display higher photocatalytic activity compared to the undoped sample, and the optimum molar ratios of Ti : Fe are found to be 100 : 1. The results reveal that the photocatalytic performance of TNT can be improved by the doping of iron ions. This may be due to the fact that a small amount of Fe^{3+} ions can act as a photo-generated hole and a photo-generated electron trap and inhibit the hole-electron recombination [22, 23]. However, when the dopant amount of Fe is too high, the photocatalytic activity decreases, despite the fact that there is still an increase in the absorbance of the visible light. This may be ascribed to three factors. One is the decreased crystallinity [8], one is the increased Fe^{3+} as a recombination center [17, 22], and the other is the decreasing separation distance of the charge carrier with the increase of Fe^{3+} content [22, 23].

It is well known that photocatalytic performance is related to the pH value of the solution [10, 28–30]. In order to obtain the optimal pH value of solution for photodegradation, we test the photocatalytic activities of Fe-TNT-1 and pure TNT in solutions of different pH values (pH = 2.1, 3.4, 4.5, 5.7, 6.6, and 7.5). The concentrations of the photocatalyst were kept at 1 g/L. All of the curves are shown in Figure 6. The

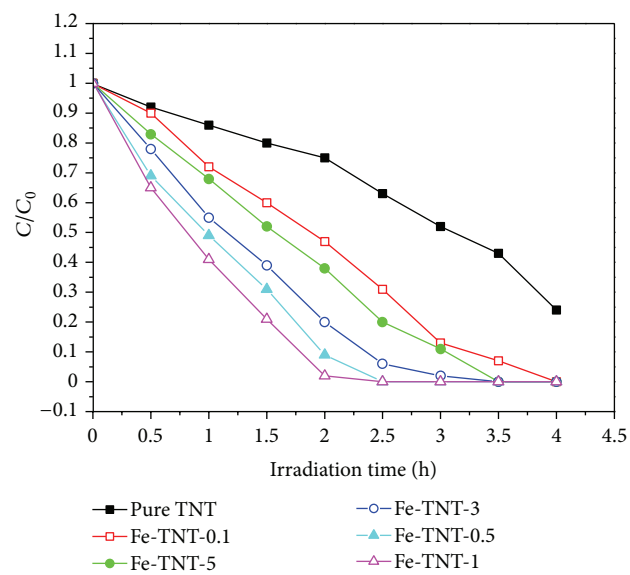

Figure 5: The photocatalytic activity of as-synthesized samples with different molar ratios of Ti : Fe under visible light irradiation.

overall activity and reaction rate constant decrease with the increase of pH. After irradiation for 0.5 h, about 73% of MO is degraded by Fe-TNT-1 when pH value was 2.1, while about 35% of MO when pH value was 7.5 in Figure 6(a). Evidently, the photodegradation was better in the acidic solution. Pure TNT revealed the similar variation trend in Figure 6(b), and others also reported similar results [31–35]. They believed that the role of pH was to tone the surface charge and band edge position of catalyst or change other physicochemical properties of the system [23, 36]. Since MO has an anionic configuration, the adsorption of MO on the Fe-doped TNT

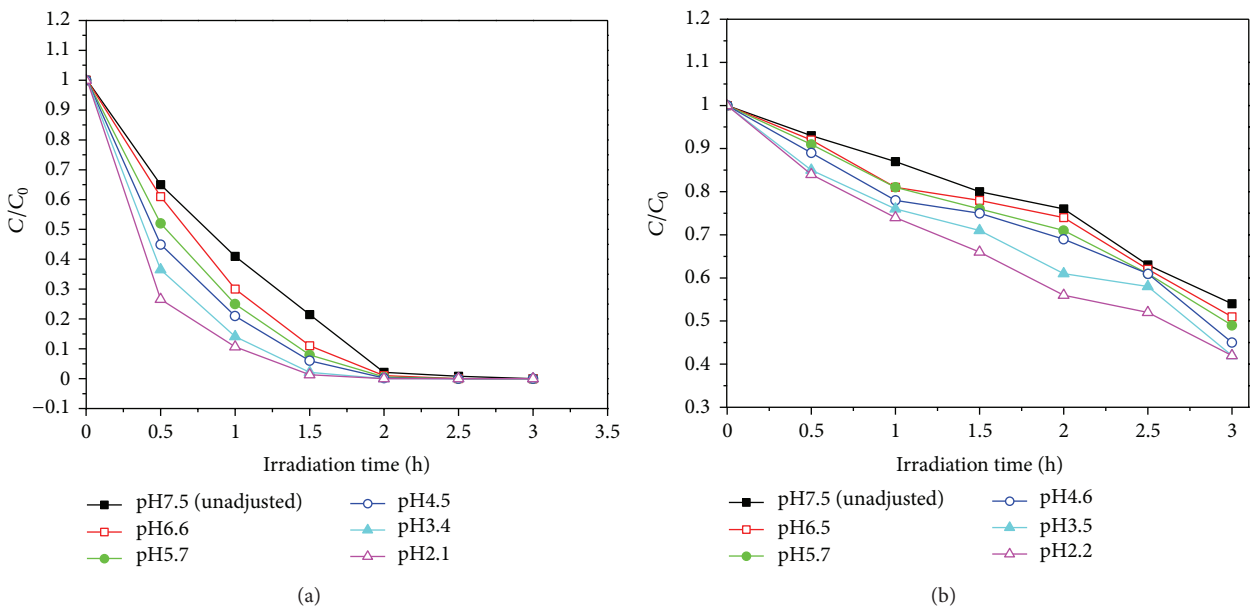

Figure 6: The photocatalytic activity of Fe-TNT-1 (a) and pure TNT (b) with different pH under visible light irradiation.

surface is favored in acidic solution. On the other hand, in the catalytic process, H^+ can enhance the surface acidity of Fe-doped TNT and promote MO molecules to interact with Fe-doped TNT. The optimum pH of solution is about 2.1 in this test.

The investigation of Fe-TNT-1 concentrations on the degradation of MO was conducted, which is shown in Figure 7. The initial pH values of MO solution are kept at 2.1. The degradation efficiency of MO increased with the increase of the concentration of Fe-TNT-1. However, the degradation efficiency changed a little when the concentration of Fe-doped TNT was more than 1.0 g/L. This can be explained on the basis that optimum photocatalyst loading is dependent on initial solute concentration. If the concentration of photocatalyst was increased, the total active surface would increase correspondingly, and as a result, the enhanced photocatalytic performance was obtained. However, the increased concentration of photocatalyst would have no effect on promoting the degradation efficiency after a maximum photocatalyst concentration was imposed. This may be ascribed to the increased aggregation of photocatalyst at high concentration [30, 36].

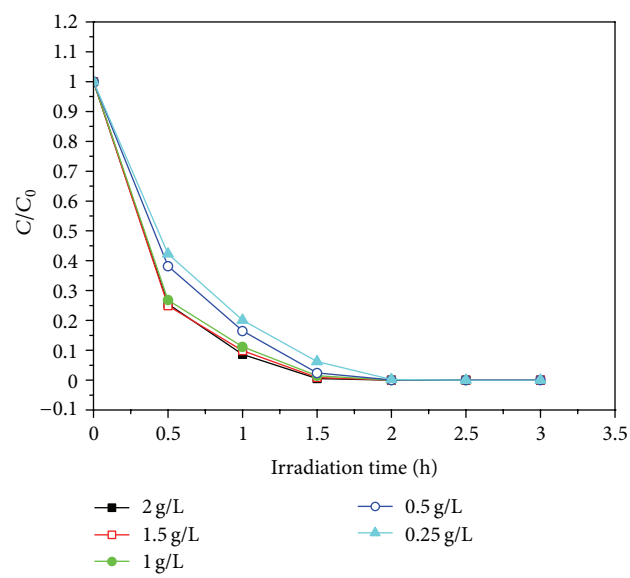

Figure 7: The photocatalytic activity of Fe-TNT-1 with different dosages under visible light irradiation.

3.3. Photocatalyst Stability. Titanium dioxide has the features of resistance to photocorrosion, which is one of the reasons of titanium dioxide as photocatalyst. If that photocorrosion of Fe-doped TNT happens, is probably the depositional Fe corrosion by dissolutions of Fe^{2+} and Fe^{3+} in solution. Therefore, we researched the dissolutions of Fe with MO degradation with atomic absorption spectrometry. After 72 h of continuous illumination experiments, not checking out the iron ions in the solution, it is shown that Fe-doped TNT has the features of resistance to photocorrosion. In order to further investigate stability of Fe-doped TNT, separation and recycling of Fe-doped TNT have been repeated for dealing with MO solution. The results were shown in Figure 8. A catalytic effect is basically unchanged after being used for 20 times repeatedly. The catalyst showed stable performance.

4. Conclusions

Fe-doped titanate nanotubes are prepared by the sonication-hydrothermal treatment. The investigation shows that the incorporation of Fe into the TiO_2 lattice accelerates decreases the crystallinity. The length of nanotubes is more than

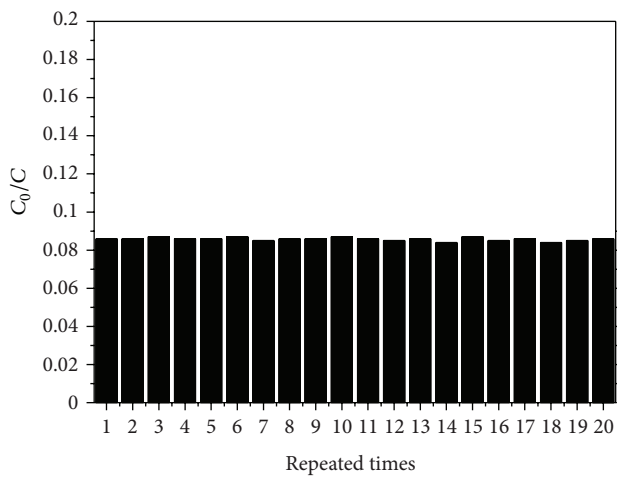

Figure 8: The reusability of the catalyst (20 mg/L of MO aqueous solution, initial pH = 2.1, 1.0 g/L of Fe-TNT-1, illumination 1 hour).

hundreds of nanometers. Most of the nanotubes keep their tubular texture after the calcination process. Increasing the amount of Fe also results in a decrease in the energy band gap and an enhanced absorption in the visible region. Doping an appropriate amount of Fe, the TiO_2 nanotube shows improved photocatalytic activity under visible light. The prepared Fe-doped TNT may be promising for practical application in the field of visible light photocatalysis. The catalyst has also the advantages of easy recovery, can maintain a higher activity after a plurality of repeated uses, and has higher industrial application value.

Acknowledgments

The authors greatly acknowledge the financial support obtained from the National Natural Science Foundation of China (no. 21077041) and the Science Foundation of Jilin Province of China (no. 201205076).

References

[1] J. C. Colmenares, R. Luque, J. M. Campelo, F. Colmenares, Z. Karpinski, and A. A. Romero, "Nanostructured photocatalysts and their applications in the photocatalytic transformation of lignocellulosic biomass: an overview," *Materials*, vol. 2, no. 4, pp. 2228–2258, 2009.

[2] J. M. Peralta-Hernández, J. Manríquez, Y. Meas-Vong et al., "Photocatalytic properties of nano-structured TiO_2-carbon films obtained by means of electrophoretic deposition," *Journal of Hazardous Materials*, vol. 147, no. 1-2, pp. 588–593, 2007.

[3] D. M. Metzler, M. Li, A. Erdem, and C. P. Huang, "Responses of algae to photocatalytic nano-TiO_2 particles with an emphasis on the effect of particle size," *Chemical Engineering Journal*, vol. 170, no. 2-3, pp. 538–546, 2011.

[4] S.-Y. Lu, D. Wu, Q.-L. Wang, J. Yan, A. G. Buekens, and K.-F. Cen, "Photocatalytic decomposition on nano-TiO_2: destruction of chloroaromatic compounds," *Chemosphere*, vol. 82, no. 9, pp. 1215–1224, 2011.

[5] M. Y. Ghaly, T. S. Jamil, I. E. El-Seesy, E. R. Souaya, and R. A. Nasr, "Treatment of highly polluted paper mill wastewater by solar photocatalytic oxidation with synthesized nano TiO_2," *Chemical Engineering Journal*, vol. 168, no. 1, pp. 446–454, 2011.

[6] J. Gao, X. Tan, Y. Miao, and R. Xin, "Modification of rutile nano-TiO_2 powders with visible light photocatalytic activity in hydrogen or nitrogen atmosphere," *Integrated Ferroelectrics*, vol. 129, no. 1, pp. 169–175, 2011.

[7] C. L. Wong, Y. N. Tan, and A. R. Mohamed, "A review on the formation of titania nanotube photocatalysts by hydrothermal treatment," *Journal of Environmental Management*, vol. 92, no. 7, pp. 1669–1680, 2011.

[8] Y.-F. Tu, S.-Y. Huang, J.-P. Sang, and X.-W. Zou, "Preparation of Fe-doped TiO_2 nanotube arrays and their photocatalytic activities under visible light," *Materials Research Bulletin*, vol. 45, no. 2, pp. 224–229, 2010.

[9] C.-C. Hu, T.-C. Hsu, and L.-H. Kao, "One-step cohydrothermal synthesis of nitrogen-doped titanium oxide nanotubes with enhanced visible light photocatalytic activity," *International Journal of Photoenergy*, vol. 2012, Article ID 391958, 9 pages, 2012.

[10] X. Zhou, F. Peng, H. Wang, H. Yu, and J. Yang, "Preparation of B, N-codoped nanotube arrays and their enhanced visible light photoelectrochemical performances," *Electrochemistry Communications*, vol. 13, no. 2, pp. 121–124, 2011.

[11] X. Zhang, L. Lei, J. Zhang, Q. Chen, J. Bao, and B. Fang, "A novel CdS/S-TiO_2 nanotubes photocatalyst with high visible light activity," *Separation and Purification Technology*, vol. 66, no. 2, pp. 417–421, 2009.

[12] M. Alam Khan, M. Shaheer Akhtar, S. I. Woo, and O.-B. Yang, "Enhanced photoresponse under visible light in Pt ionized TiO_2 nanotube for the photocatalytic splitting of water," *Catalysis Communications*, vol. 10, no. 1, pp. 1–5, 2008.

[13] G. An, W. Ma, Z. Sun et al., "Preparation of titania/carbon nanotube composites using supercritical ethanol and their photocatalytic activity for phenol degradation under visible light irradiation," *Carbon*, vol. 45, no. 9, pp. 1795–1801, 2007.

[14] C. Feng, J. Zhang, R. Lang, Z. Jin, Z. Wu, and Z. Zhang, "Unusual photo-induced adsorption-desorption behavior of propylene on Ag/TiO_2 nanotube under visible light irradiation," *Applied Surface Science*, vol. 257, no. 6, pp. 1864–1870, 2011.

[15] M. A. Khan and O.-B. Yang, "Photocatalytic water splitting for hydrogen production under visible light on Ir and Co ionized titania nanotube," *Catalysis Today*, vol. 146, no. 1-2, pp. 177–182, 2009.

[16] Y.-K. Lai, J.-Y. Huang, H.-F. Zhang et al., "Nitrogen-doped TiO_2 nanotube array films with enhanced photocatalytic activity under various light sources," *Journal of Hazardous Materials*, vol. 184, no. 1–3, pp. 855–863, 2010.

[17] L. Deng, S. Wang, D. Liu et al., "Synthesis, characterization of Fe-doped TiO_2 nanotubes with high photocatalytic activity," *Catalysis Letters*, vol. 129, no. 3-4, pp. 513–518, 2009.

[18] Z. Zhang, M. F. Hossain, and T. Takahashi, "Self-assembled hematite (α-Fe_2O_3) nanotube arrays for photoelectrocatalytic degradation of azo dye under simulated solar light irradiation," *Applied Catalysis B*, vol. 95, no. 3-4, pp. 423–429, 2010.

[19] L. Sun, J. Li, C. L. Wang, S. F. Li, H. B. Chen, and C. J. Lin, "An electrochemical strategy of doping Fe^{3+} into TiO_2 nanotube array films for enhancement in photocatalytic activity," *Solar Energy Materials and Solar Cells*, vol. 93, no. 10, pp. 1875–1880, 2009.

[20] Q. Wu, J. Ouyang, K. Xie, L. Sun, M. Wang, and C. Lin, "Ultrasound-assisted synthesis and visible-light-driven photocatalytic activity of Fe-incorporated TiO_2 nanotube array photocatalysts," *Journal of Hazardous Materials*, vol. 199-200, pp. 410–417, 2012.

[21] Z. Xu and J. Yu, "Visible-light-induced photoelectrochemical behaviors of Fe-modified TiO_2 nanotube arrays," *Nanoscale*, vol. 3, no. 8, pp. 3138–3144, 2011.

[22] S. K. Mohapatra, S. Banerjee, and M. Misra, "Synthesis of Fe_2O_3/TiO_2 nanorod-nanotube arrays by filling TiO_2 nanotubes with Fe," *Nanotechnology*, vol. 19, no. 31, Article ID 315601, 2008.

[23] H. An, J. Li, J. Zhou, K. Li, B. Zhu, and W. Huang, "Iron-coated TiO_2 nanotubes and their photocatalytic performance," *Journal of Materials Chemistry*, vol. 20, no. 3, pp. 603–610, 2010.

[24] Y. Ma, Y. Lin, X. Xiao, X. Zhou, and X. Li, "Sonication-hydrothermal combination technique for the synthesis of titanate nanotubes from commercially available precursors," *Materials Research Bulletin*, vol. 41, no. 2, pp. 237–243, 2006.

[25] Z. Ambrus, N. Balázs, T. Alapi et al., "Synthesis, structure and photocatalytic properties of Fe(III)-doped TiO_2 prepared from $TiCl_3$," *Applied Catalysis B*, vol. 81, no. 1-2, pp. 27–37, 2008.

[26] W.-C. Hung, S.-H. Fu, J.-J. Tseng, H. Chu, and T.-H. Ko, "Study on photocatalytic degradation of gaseous dichloromethane using pure and iron ion-doped TiO_2 prepared by the sol-gel method," *Chemosphere*, vol. 66, no. 11, pp. 2142–2151, 2007.

[27] X. Liu, M. K. Devaraju, S. Yin et al., "The preparation and characterization of tabular, pearlescent Fe-doped potassium lithium titanate," *Dyes and Pigments*, vol. 84, no. 3, pp. 237–241, 2010.

[28] W.-Y. Zhou, S.-Q. Tang, Z.-B. Wei, Y.-H. Xu, and Q.-M. Lu, "Effects of heat treatment and atmosphere on the visible light photocatalytic activity of nano-TiO_2," *Journal of Inorganic Materials*, vol. 23, no. 1, pp. 61–65, 2008.

[29] Y. Zhao, X. Zhang, J. Zhai et al., "Enhanced photocatalytic activity of hierarchically micro-/nano-porous TiO_2 films," *Applied Catalysis B*, vol. 83, no. 1-2, pp. 24–29, 2008.

[30] X. Zhao, L. Zhu, Y. Zhang et al., "Removing organic contaminants with bifunctional iron modified rectorite as efficient adsorbent and visible light photo-Fenton catalyst," *Journal of Hazardous Materials*, vol. 215-216, pp. 57–64, 2012.

[31] R. Vargas and O. Núñez, "The photocatalytic oxidation of dibenzothiophene (DBT)," *Journal of Molecular Catalysis A*, vol. 294, no. 1-2, pp. 74–81, 2008.

[32] C. Karunakaran and R. Dhanalakshmi, "Semiconductor-catalyzed degradation of phenols with sunlight," *Solar Energy Materials and Solar Cells*, vol. 92, no. 11, pp. 1315–1321, 2008.

[33] E. Grabowska, J. W. Sobczak, M. Gazda, and A. Zaleska, "Surface properties and visible light activity of W-TiO_2 photocatalysts prepared by surface impregnation and sol-gel method," *Applied Catalysis B*, vol. 117-118, pp. 351–359, 2012.

[34] K. L. Schulte, P. A. DeSario, and K. A. Gray, "Effect of crystal phase composition on the reductive and oxidative abilities of TiO_2 nanotubes under UV and visible light," *Applied Catalysis B*, vol. 97, no. 3-4, pp. 354–360, 2010.

[35] N. Wang, L. Zhu, K. Deng, Y. She, Y. Yu, and H. Tang, "Visible light photocatalytic reduction of Cr(VI) on TiO_2 in situ modified with small molecular weight organic acids," *Applied Catalysis B*, vol. 95, no. 3-4, pp. 400–407, 2010.

[36] Y. Chen, Y. Zhang, C. Liu, A. Lu, and W. Zhang, "Photodegradation of malachite green by nanostructured Bi_2WO_6 visible light-induced photocatalyst," *International Journal of Photoenergy*, vol. 2012, Article ID 510158, 6 pages, 2012.